

Advanced intelligent Clear-IQ Engine (AiCE) Deep Learning Reconstruction for PET Imaging with Cartesion Prime Digital PET/CT

Bing Bai, Ph.D., DABSNM
Medical Affairs Manager
Molecular Imaging
Canon Medical Systems USA

Maria Iatrou, Ph.D., MBA
Medical Affairs Leader
Molecular Imaging
Canon Medical Systems USA

Introduction

Cartesion Prime PET/CT, a new premium digital PET scanner by Canon Medical Systems, enables health care providers to better navigate to personalized care. Founded on an innovative SiPM-based detector design (Figure 1), Cartesion Prime provides excellent performance and return on investment. One-to-one coupling, 100% of crystal coverage, large axial FOV, fast TOF resolution, and advanced reconstruction methods which results in high quality images that can help clinicians perform clinical tasks confidently and accurately. Design choices not only optimize image quality,

but also scan times, throughput, and injected tracer dosage*, resulting in streamlined and efficient workflow.

Following the successful introduction of Advanced intelligent Clear-IQ Engine (AiCE) Deep Learning Reconstruction (DLR) technology** for CT¹ and MR, Canon Medical is now introducing this innovative technology on Cartesion Prime (Figure 2). AiCE which harnesses the enormous computational power of Deep Convolutional Neural Networks (DCNN) to deliver sharp, clear, high quality PET and CT images with improved image quality under a wide variety of imaging conditions.

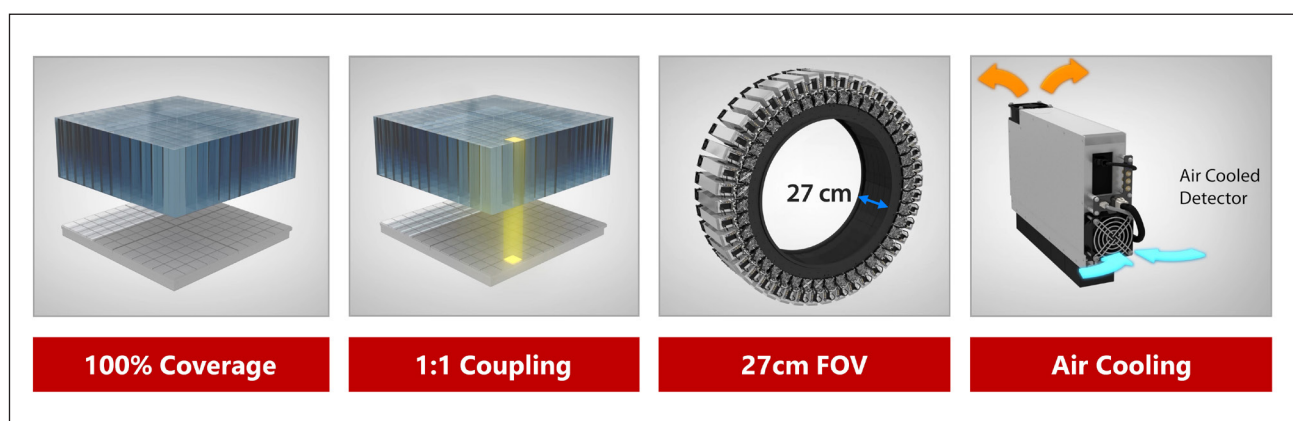


Figure 1 Cartesion Prime PET/CT: a premium system with a well-balanced digital PET detector design.

*Optimization of tracer dosage is only recommended within the dosing ranges that appear in approved PET imaging agent labeling.

**Optional

Advanced intelligent Clear-IQ Engine (AiCE) for PET

Overview

The growing role of PET imaging in the standard-of-care and the evolution of precision medicine is enabled by continuous advances in PET technology that aim to improve image quality, quantification, and clinical workflow. Despite all the advancements, PET imaging remains challenging due to a variety of factors confounding image quality. These factors include acquisition durations which are practical in clinical settings, dosages of injected radioactive tracers that are both safe for the patient and the operators, uptake times, and patients' BMI and glucose levels.

Several reconstruction methods have been developed to address the effects of these factors on PET image quality and to suppress noise. The widely (clinically adopted) ordered subset expectation maximization (OSEM) iterative reconstruction with Gaussian post-filtering, regularized reconstruction² and post-reconstruction denoising³ are among these methods. These approaches use one or more parameters to optimize signal-to-noise ratio (SNR) and/or heuristically designed functions to differentiate signal and noise.

However, optimization of parameter selection for a wide range of signal-to-noise ratios and noise magnitude makes the implementation of these approaches cumbersome. Furthermore, statistical reconstruction and smoothing techniques may affect the noise correlation of neighboring pixels, often introducing undesirable blocky noise texture or piece-wise smoothness.

Recently, deep learning convolutional neural networks (DCNN) have been proposed for image denoising.⁴ These methods optimize a large number of filters/kernels during a training process to effectively differentiate signal from noise. During training, DCNNs learn the differences between a large number of high-quality images and their noisy pairs. Canon Medical is on the forefront of DCNN-based DLR development for medical imaging as evident by the successful release of AiCE for the CT and MR product portfolios. And now, AiCE for PET* is available on Cartesion Prime to help clinicians achieve high quality images with low noise consistently, routinely and automatically across patients. Finally, AiCE for PET may potentially provide flexibility to clinicians to reduce counts, or equivalently PET acquisition duration while preserving SNR at levels achieved by OSEM with point spread function (PSF) and Gaussian post-filtering without any reduction.

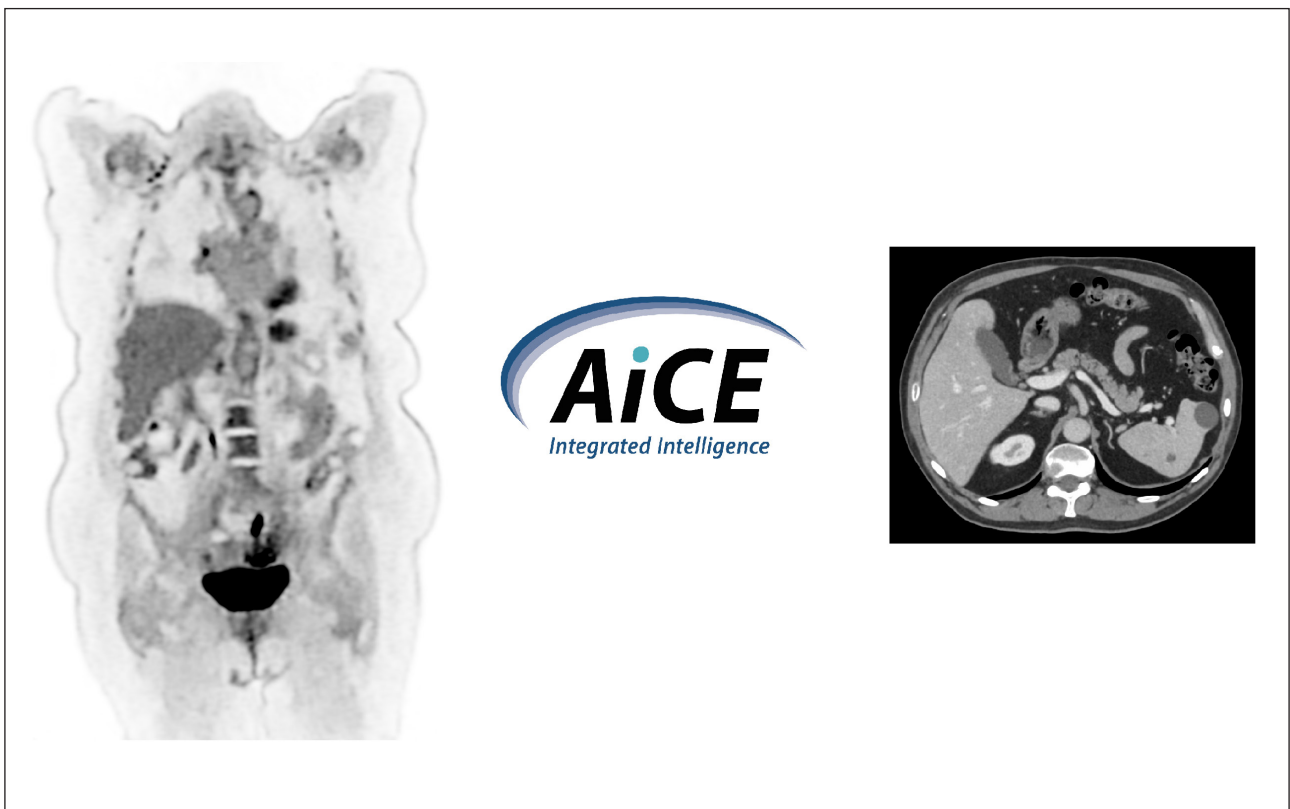


Figure 2 Cartesion Prime powered by AiCE Deep Learning Reconstruction both for PET and CT.

*Option

Training

Cartesion Prime's AiCE DCNN for PET is based on a multi-layer residual network architecture.⁵ The training is performed by feeding the network batches of noisy data along with each corresponding high-quality image (Figure 3). The high-quality images are called "targets" and can be generated from longer acquisition or higher-dose PET data. During the training process, AiCE for PET optimizes iteratively and automatically the filters/kernels of its DCNN layers to minimize the differences between training samples (noisy data) and their paired training targets. The trained DCNN can be applied to new data to output a new, high-quality image that resembles the noise level of the target images (labels) used for training. Cartesion Prime AiCE for PET was trained

using high-quality datasets as targets that were acquired during longer than typical clinical protocols. The list-mode data corresponding to the longer acquisitions were uniformly parsed (down-sampled) into smaller list-mode data sets, simulating scans with shorter acquisition durations and, equivalently, lower count levels. These down-sampled training datasets, therefore, represented datasets at different noise levels. In the training process, all the inputs at the different noise levels are paired with the same high-quality target (Figure 4). Consequently, the DCNN can learn to adapt to different noise levels automatically to yield low noise high-quality PET images. This complex training process is completed during the development phase and no training takes place after the deployment of AiCE at clinical sites.

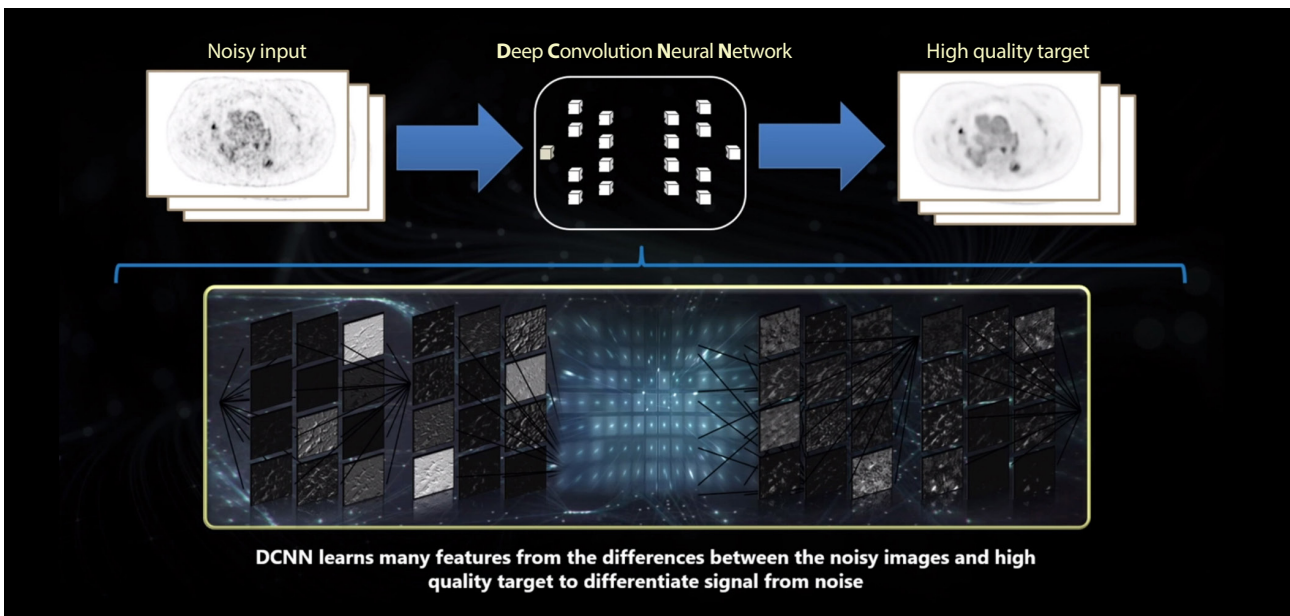


Figure 3 AiCE DLR for PET utilizing DCNN is trained with high quality Target Images and learns to turn low-quality input data into low-noise images that are sharp and clear.

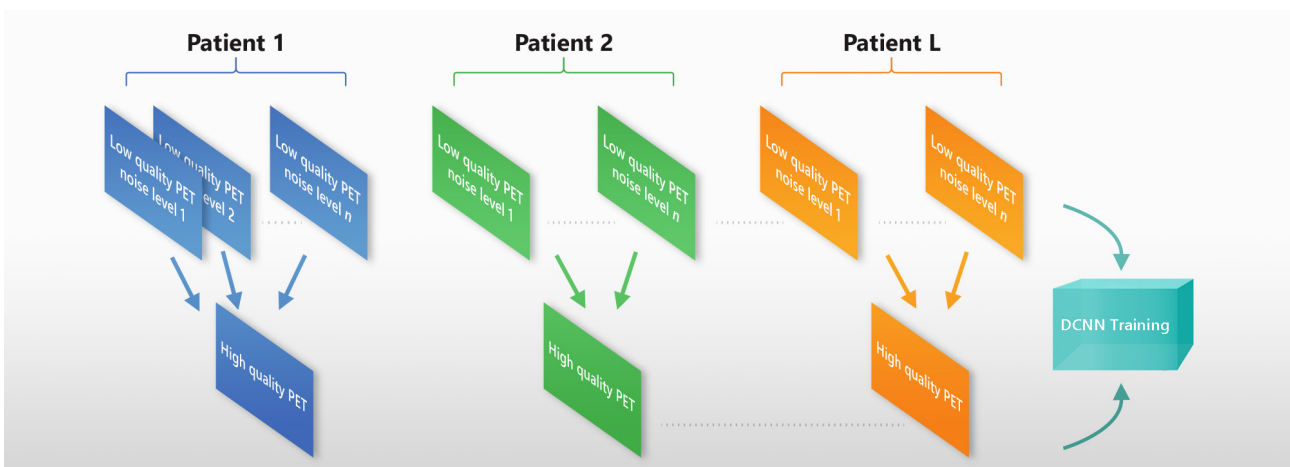


Figure 4 Lower quality PET data-sets at different noise levels were paired with the same high-quality target. Consequently, the DCNN can learn to adapt to different noise levels automatically to yield low-noise high-quality PET images.

*Option

Performance

AiCE for PET yields superior performance compared to Gaussian post-filtered OSEM by better differentiating signal from noise while generating high-quality images. Canon has performed phantom studies to evaluate image quality, quantification accuracy, preservation of SNR at reduced counts, or equivalently scan duration, and preservation of quantification. Table 1 summarizes the performance comparison.

Table 1 Summary of performance improvement of AiCE for PET compared to Gaussian post-filtered OSEM.

AiCE for PET IQ Improvements	
SNR	45%
CRC	82.9%
Counts/Scan Time	75%
Preservation of Quantification	Yes

Image quality

Image quality was evaluated following the NEMA NU 2 standard.^{6,7} A NEMA image quality phantom with hot-to-background ratio of 4:1 was scanned on a Cartesian Prime scanner for three beds at four minutes per bed. The experiment was repeated 10 times and the results reported in this section are mean values. The data was reconstructed using AiCE for PET and a clinical protocol, which is OSEM with point-spread-function (PSF), 4 iterations, 12 subsets, and a 6 mm full-width-at-half-maximum (FWHM) Gaussian post-filter. We measured the SNR, which is defined as the ratio of the region of interest (ROI) mean of the hot sphere (10 mm) to the background variability (BGV). Results in Table 2 showed that AiCE can improve SNR by 45% compared to OSEM + Gaussian post-filter.

Table 2 SNR of 10 mm sphere reconstructed using AiCE for PET and OSEM+PSF+Gaussian from 10 experiments.

SNR	AiCE	GF6mm	% Diff
Average	89.15	61.47	45.03%
Std Error	3.61	2.94	NA

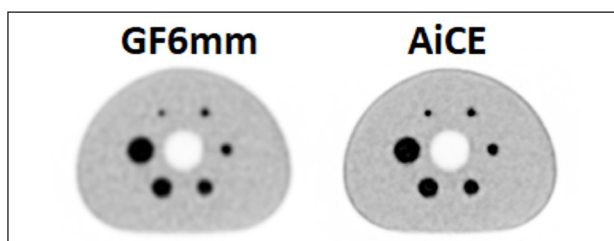


Figure 5 NEMA image quality phantom reconstructed using AiCE and clinical protocol (OSEM+PSF 4 iterations, 12 subsets, 6 mm FWHM Gaussian post-filter).

Quantification accuracy

The NEMA image quality phantom data used for image quality measurement in the previous section was reconstructed using OSEM with PSF, 4 iterations, 12 subsets, and smoothed using Gaussian post-filter with different FWHM. The contrast recovery coefficient (CRC) of the 10 mm diameter sphere was compared between AiCE and OSEM+PSF+Gaussian filter at equivalent noise, as expressed by background variability (BGV). Results showed an 82.9% improvement in contrast at the same noise level (BGV) compared to OSEM with Gaussian post-filtering. BGV between AiCE and OSEM+PSF+Gaussian filter was equivalent for a Gaussian filter at 6mm FWHM.

Table 3 CRC and BGV of 10mm sphere reconstructed using AiCE for PET and OSEM+PSF+Gaussian from 10 experiments.

		AiCE	GF6mm	% Diff
CRC (Q ₁₀)	Average	68.13	37.25	82.9%
	Std Error	1.67	0.63	NA
BGV (N ₁₀)	Average	3.53	3.58	-1.4%
	Std Error	0.13	0.15	NA

Count dependency

Bench test results demonstrated that AiCE for PET can preserve SNR while significantly reducing counts, or equivalently scan duration, compared to OSEM with PSF and Gaussian post-filtering. A NEMA image quality phantom study showed that counts can be reduced with AiCE by 75% while preserving the SNR achieved with OSEM with Gaussian post-filtering at 100% counts or without scan duration reduction.

Table 4 SNR of 10mm sphere reconstructed using AiCE for PET and OSEM+PSF+Gaussian from 1 min/bed and 4 min/bed data (10 experiments).

	Duration [min/bed]	SNR	
		1	4
AiCE	Average	62.77	89.15
	Std Error	2.22	3.61
Gaussian 6mm	Average	35.57	61.47
	Std Error	1.19	2.94

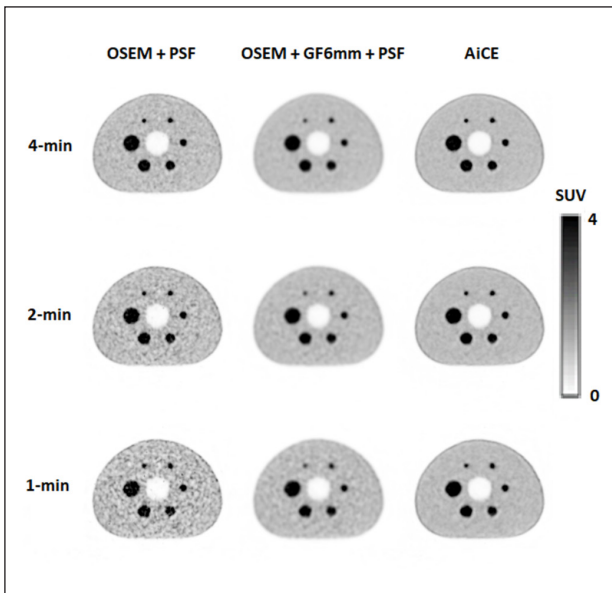


Figure 6 NEMA image quality phantom reconstructed using AiCE and OSEM+PSF+Gaussian at: 4, 2, and 1 min/bed.

Preservation of quantification

Overall quantification of the image was evaluated using the NEMA image quality data. Background mean SUV, average SUV at the center slice, and average SUV of the entire phantom in the AiCE image were measured and compared with the respective OSEM+PSF+Gaussian image. Results showed that AiCE did not change the overall quantification of reconstructed image.

Clinical studies

Whole body PET

a) Large BMI with low contrast lesion.

Figure 7 shows the whole body ^{18}F -FDG images of a large patient (BMI 39.2) with primary lung adenocarcinoma and DCIS of right breast. Patient was injected with 266 MBq (7.2 mCi) of ^{18}F -FDG and was scanned on a Cartesion

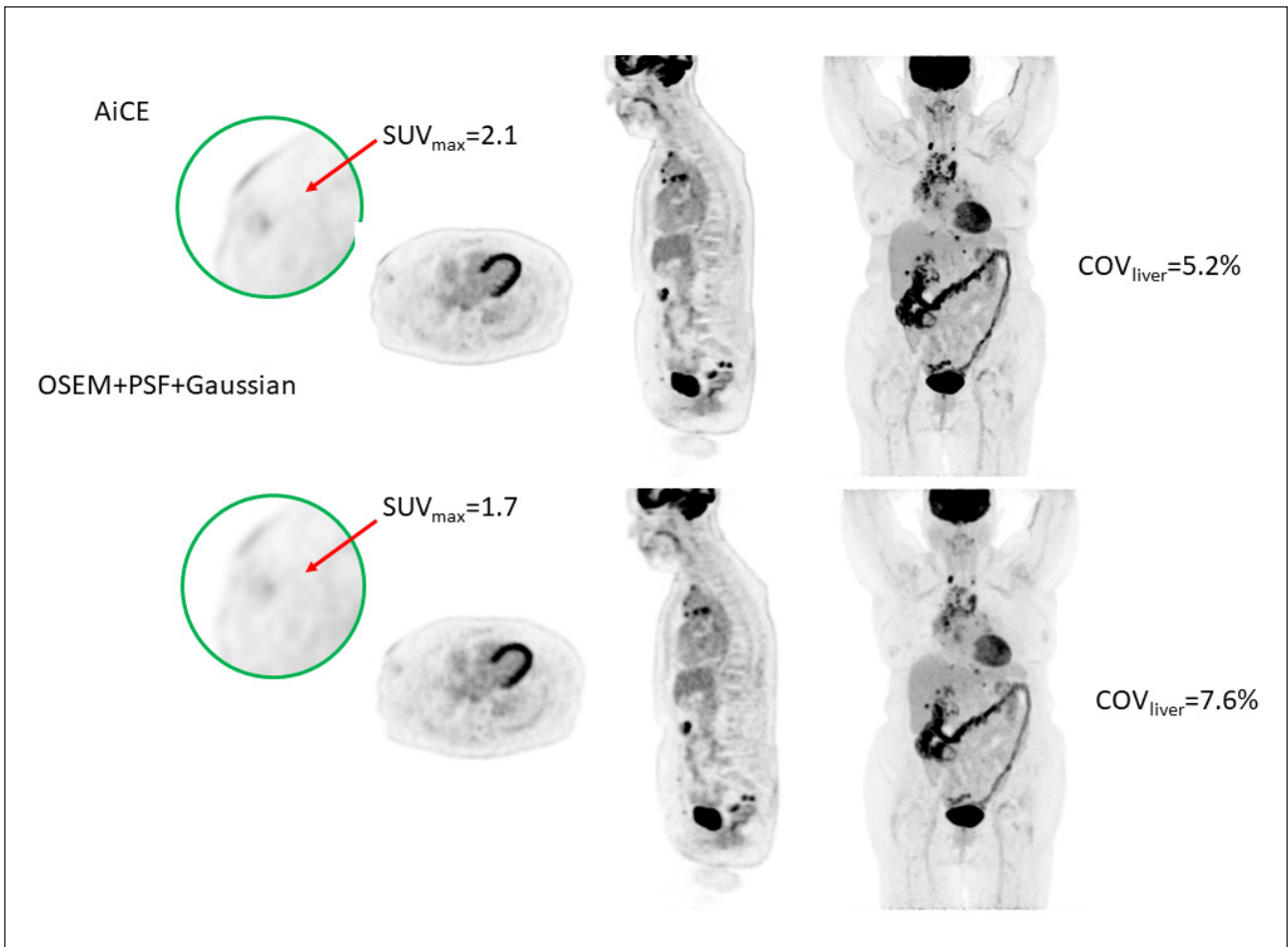


Figure 7 AiCE and OSEM+PSF+Gaussian images of a patient with large BMI and a low contrast lesion in the outer right breast shown in the zoom-in image.

Prime PET/CT after 53 minutes. The scan protocol comprised 5 beds with 2 minutes per bed and 50% bed overlap. The image was reconstructed using AiCE and OSEM with PSF, 4 iterations and 12 subsets, followed by a Gaussian filter with 6 mm FWHM. AiCE image shows improved sharpness of the low contrast lesion in the outer right breast and multiple clusters of mediastinal lymph nodes. SUVmax of the low contrast lesion in the right breast is increase by 23% in AiCE (2.1) compared to OSEM+PSF+Gaussian (1.7). A spherical ROI with diameter of 3 cm was drawn in the center of the liver and we measured the coefficient of variation (COV), which is defined by the ratio of standard deviation and the mean of the ROI. The COV of the liver ROI is decreased by 32% in AiCE (5.2%) compared to OSEM+PSF+Gaussian (7.6%).

b) Breast cancer

Figure 8 shows the whole body ¹⁸F-FDG images of a patient (BMI 19.4) with breast cancer. Patient was injected

with 281 MBq (7.6 mCi) of ¹⁸F-FDG and waited for 62 minutes before being scanned on a Cartesion Prime PET/CT for 5 beds with 2 minutes per bed and 50% bed overlap. Images were reconstructed using AiCE and OSEM with PSF, 4 iterations and 12 subsets, followed by a Gaussian filter with 6 mm FWHM. AiCE image shows easier detection of a sub-centimeter left chest wall nodule and better definition of pleural metastatic disease. A spherical ROI with diameter of 3 cm was drawn in the center of the liver. The liver of AiCE image is less noisy compared to OSEM+PSF+Gaussian image, as shown by the reduced COV of liver ROI measured.

c) Colon cancer with small lesions

Figure 9 shows the whole body ¹⁸F-FDG images of a patient (BMI 22.6) with colon cancer. Patient was injected with 278 MBq (7.5 mCi) of ¹⁸F-FDG and waited for 56 minutes before being scanned on a Cartesion Prime PET/CT for 5 beds with 2 minutes per bed and 50% bed

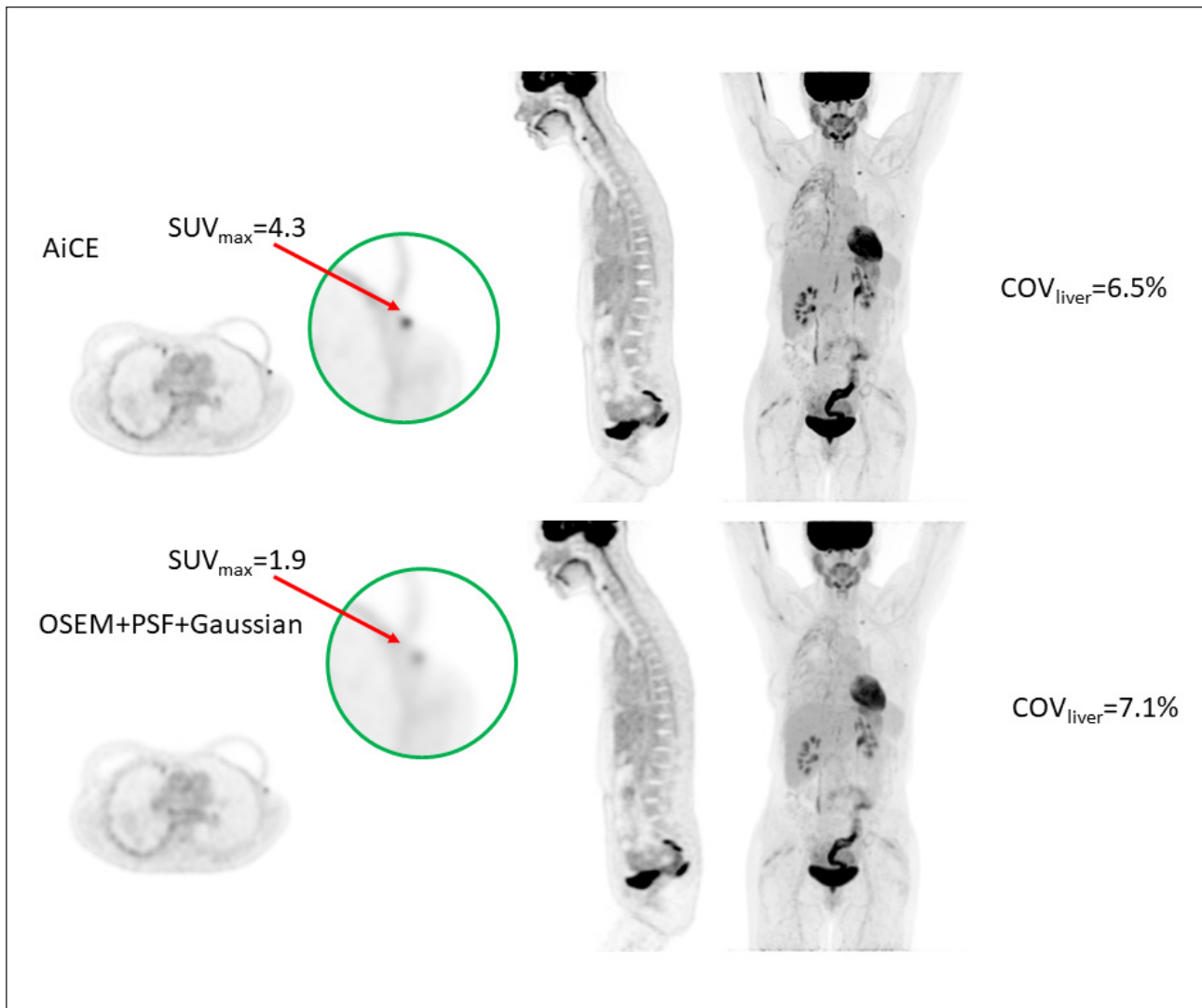


Figure 8 AiCE and OSEM+PSF+Gaussian SEM images of a breast cancer patient. A left chest wall nodules is shown in the zoom-in image.

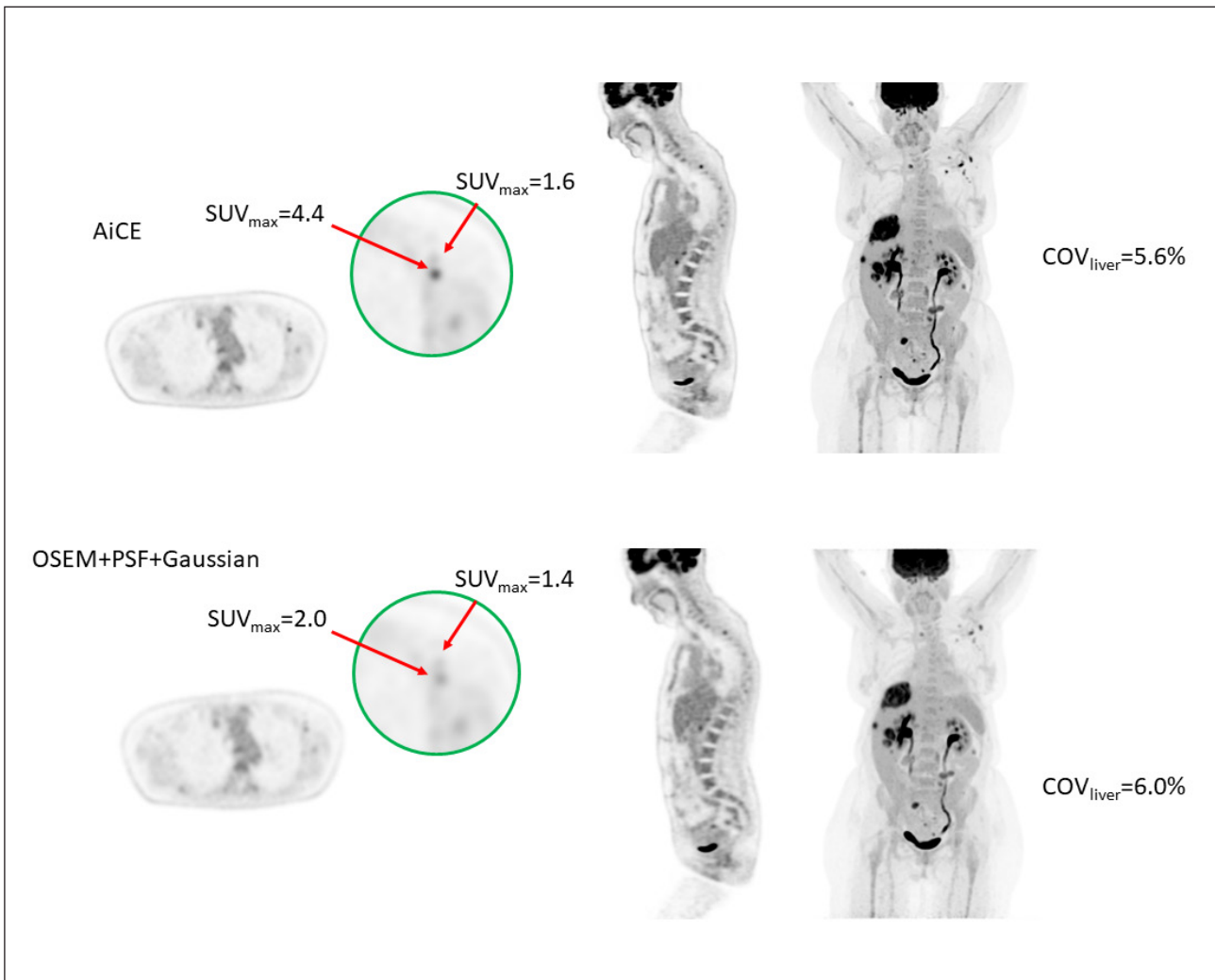


Figure 9 AiCE and OSEM+PSF+Gaussian images of a colon cancer patient with small lesions. Two adjacent sub-centimeter left axillary lymph nodes are shown in the zoom-in image.

overlap. Images were reconstructed using AiCE and OSEM with PSF, 4 iterations and 12 subsets, followed by a Gaussian filter with 6 mm FWHM. The AiCE image is sharper, which allows better definition of the small left axillary lymph nodes. Two adjacent lymph nodes are shown in Figure 9. The AiCE image shows better contrast and separation of the two nodes. A spherical ROI with diameter of 3 cm was drawn in the center of the liver region with normal uptake. The AiCE image has less noise in the liver than OSEM+PSF+Gaussian image, as shown by the reduced COV in the liver ROI.

Reduced scan time per bed position

Figure 10 shows the whole body ¹⁸F-FDG images of a patient (BMI 19.8) with lung cancer. Patient was injected with 289 MBq (7.8 mCi) of ¹⁸F-FDG and waited for 58 minutes before moving to Cartesian Prime PET/CT for a scan, comprising 5 beds with 2 minutes per bed and 50% bed overlap. Images were reconstructed using AiCE and OSEM with PSF, 4 iterations and 12 subsets, followed by a

Gaussian filter with 6 mm FWHM. In addition, the listmode file was resampled to extract 75% and 50% of the counts, which correspond to 90 and 60 seconds per bed respectively. The down-sampled data was reconstructed using AiCE and OSEM+PSF+Gaussian with the same parameters as described above.

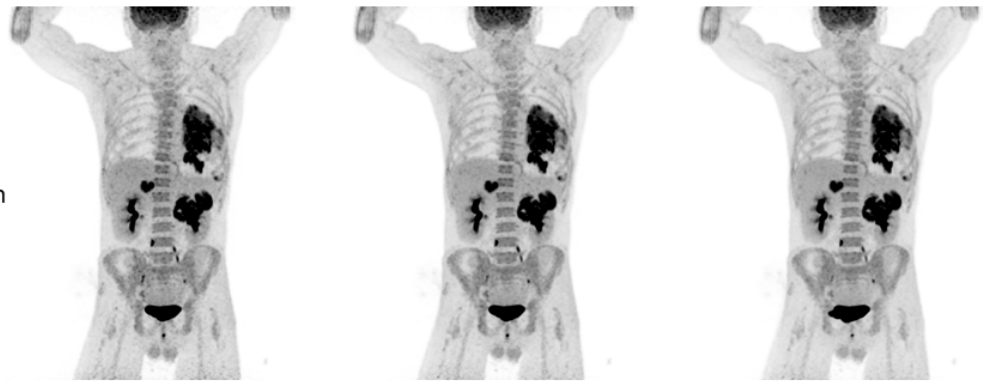
The AiCE image shows better visualization of normal physiological uptake in the vertebral body. There are two sub-centimeter nodules in the left upper lobe lung, which show improved sharpness in the AiCE image. The AiCE images reconstructed from less data show similar noise as the full count data, while OSEM+PSF+Gaussian images show higher noise when reconstructed from less data. A spherical ROI with diameter of 3 cm was drawn in the center of the liver. The COV of the liver ROI increased by 15% when the scan time was reduced from 120 sec/bed (7.3%) to 60 sec/bed (8.4%) and then reconstructed with the AiCE image. For OSEM+PSF+Gaussian image, the COV of liver ROI increased by 73% when the scan time was reduced from 120 sec/bed (7.1%) to 60 sec/bed (12.3%).

a)

AiCE



OSEM+PSF+Gaussian



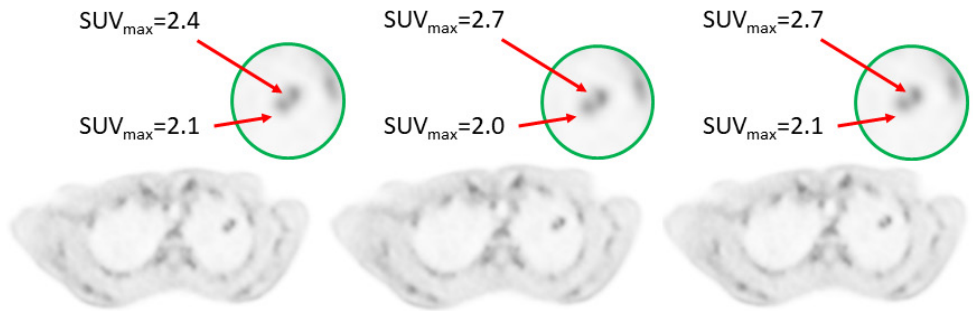
60 sec/bed

90 sec/bed

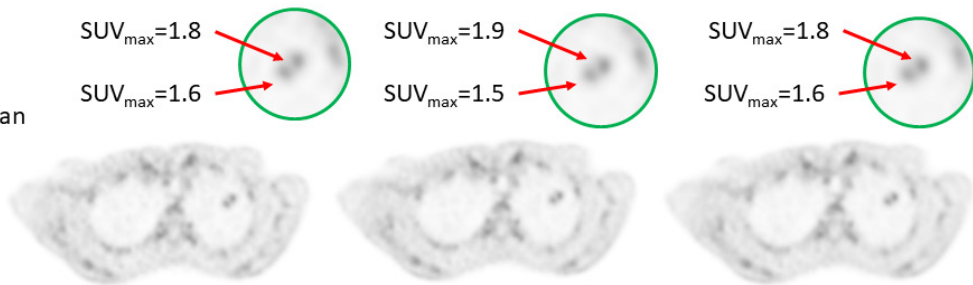
120 sec/bed

b)

AiCE



OSEM+PSF+Gaussian



60 sec/bed

90 sec/bed

120 sec/bed

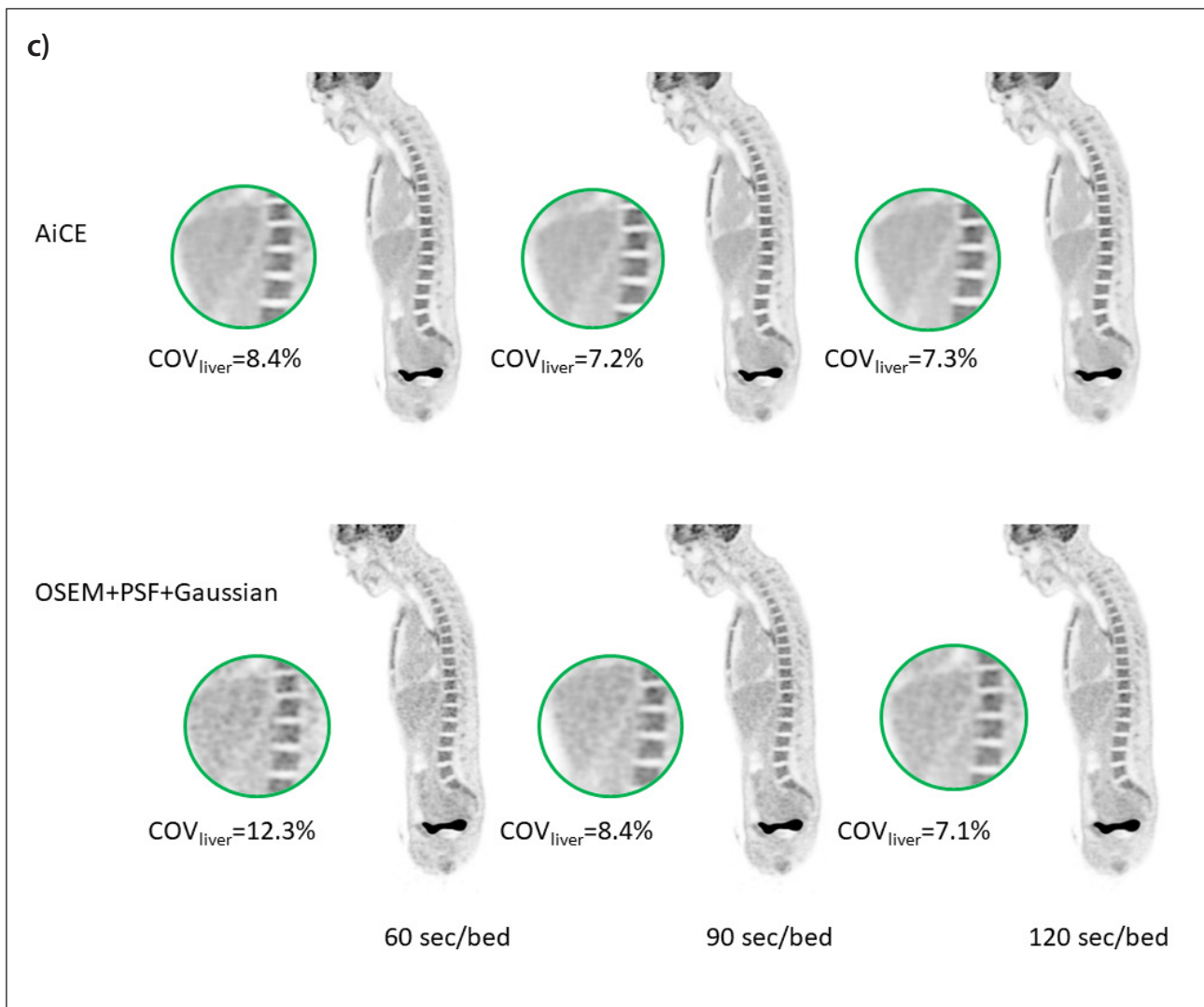


Figure 10 a) AiCE and OSEM+PSF+Gaussian images reconstructed from 50%, 75% and 100% of data, corresponding to 60, 90, and 120 sec/bed. Two adjacent sub-centimeter nodules in the left upper lobe lung are shown in the zoomed in axial slice (b), while the zoomed-in in sagittal slice (c) shows the liver.

CT: more opportunity with Aquilion Prime SP

Cartesion Prime leverages Canon’s high performance Aquilion Prime SP CT to deliver advanced PET technologies with premium CT features that come standard with every scanner. Aquilion Prime SP CT features a 78 cm CT bore and a detector with 80 rows of 0.5 mm detector elements*. Cartesion Prime is augmented by Canon’s standard diagnostic suite of CT features, including Single Energy Metal Artifact Reduction (SEMAR), AIDR 3D for fast iterative reconstruction, and PUREVision Optics for optimized imaging performance.⁸ In addition to all these features, Canon’s AiCE DLR for CT* is also available on Cartesion Prime to deliver extraordinary CT image quality.

Conclusions

Cartesion Prime digital PET/CT is now coupled with AiCE DLR both for CT and PET to help clinicians further improve image quality. AiCE for PET, the latest introduction of innovative DCNN-based DLR approaches developed by Canon Medical, is designed to automatically improve SNR and overall image quality compared to OSEM with PSF and Gaussian post-filtering without the need to tune reconstruction parameters. Finally, AiCE may potentially provide flexibility to clinicians to reduce the duration of PET scans while preserving image SNR at levels achieved by OSEM with PSF and Gaussian post-filtering without scan time reduction. Clinical evidence of this new technology will help define its full potential clinical impact on current patient care and future opportunities.

References:

1. Boedeker K., AiCE Deep Learning Reconstruction: Bringing the power of Ultra-High Resolution CT to routine imaging, Canon Medical Systems Corporation, 2019.
2. S. Ahn, S. G. Ross, E. Asma, J. Miao, X. Jin, L. Cheng, S. D. Wollenweber, and R. M. Manjeshwar, "Quantitative comparison of OSEM and penalized likelihood image reconstruction using relative difference penalties for clinical PET," *Phy. Med. Bio.*, vol. 60, pp. 5733-5751, 2016.
3. C. Chan, R. Fulton, R. Barnett, D. D. Feng, and S. Meikle, "Postreconstruction Nonlocal Means Filtering of Whole-Body PET With an Anatomical Prior," *IEEE Trans. Med. Imag.*, vol. 33, pp. 636-650, 2014.
4. K. Zhang, W. Zuo, Y. Chen, D. Meng, and L. Zhang, "Beyond a Gaussian Denoiser: Residual Learning of Deep CNN for Image Denoising," *IEEE Transactions on Image Processing*, vol. 26, pp. 3142-3155, 2017.
5. C. Chan, J. Zhou, L. Yang, W. Qi, J. Kolthammer, and E. Asma, "An Investigation Study of Deep Learning Convolutional Neural Network for Whole-Body PET Denoising," in *RSNA*, 2018.
6. National Electrical Manufacturers Assoc. Performance measurements of positron emission tomographs. NEMA Standards Publication NU 2-2012. Rosslyn, USA: National Electrical Manufacturers Association. 2012.
7. National Electrical Manufacturers Assoc. Performance measurements of positron emission tomographs. NEMA Standards Publication NU 2-2018. Rosslyn, USA: National Electrical Manufacturers Association. 2018.
8. Vaishnav J., PUREVISION Optics: The optimal balance between image quality and dose, Canon Medical Systems Corporation, 2019.

The clinical results described in this paper are the experience of the authors. Results may vary due to clinical setting, patient presentation and other factors.

CANON MEDICAL SYSTEMS USA, INC.

<https://us.medical.canon>

2441 Michelle Drive, Tustin, CA 92780 | 800.421.1968

©Canon Medical Systems, USA 2021. All rights reserved. Design and specifications are subject to change without notice.

Cartesion, Aquilion, ^{SURE}Position, SEMAR, coneXact and Made for Life are trademarks of Canon Medical Systems Corporation.

MIWP13835US MWPNM0003EB

Made For life